Microbiological Research 283 (2024) 127700

Contents lists available at ScienceDirect

Microbiological Research

journal homepage: www.elsevier.com/locate/micres

Identification of metabolites produced by six gut commensal Bacteroidales strains using non-targeted LC-MS/MS metabolite profiling

Maria Victoria Fernandez-Cantos [a], Ambrin Farizah Babu [b,c], Kati Hanhineva [b,c,d], Oscar P. Kuipers [a,*]

[a] Department of Molecular Genetics, Groningen Biomolecular Sciences and Biotechnology Institute, University of Groningen, Groningen, Netherlands
[b] School of Medicine, Institute of Public Health and Clinical Nutrition, University of Eastern Finland, 70211 Kuopio, Finland
[c] Afekta Technologies Ltd., Microkatu 1, Kuopio 70210, Finland
[d] Department of Life Technologies, Food Sciences Unit, University of Turku, Turku 20014, Finland

ARTICLE INFO

Keywords:
Bacteroidales
Non-targeted metabolomics
Segatella copri
Prevotella copri
Parabacteroides merdae
Amine
Collagen

ABSTRACT

As the most abundant gram-negative bacterial order in the gastrointestinal tract, Bacteroidales bacteria have been extensively studied for their contribution to various aspects of gut health. These bacteria are renowned for their involvement in immunomodulation and their remarkable capacity to break down complex carbohydrates and fibers. However, the human gut microbiota is known to produce many metabolites that ultimately mediate important microbe-host and microbe-microbe interactions. To gain further insights into the metabolites produced by the gut commensal strains of this order, we examined the metabolite composition of their bacterial cell cultures in the stationary phase. Based on their abundance in the gastrointestinal tract and their relevance in health and disease, we selected a total of six bacterial strains from the relevant genera *Bacteroides, Phocaeicola, Parabacteroides,* and *Segatella*. We grew these strains in modified Gifu anaerobic medium (mGAM) supplemented with mucin, which resembles the gut microbiota's natural environment. Liquid chromatography-tandem mass spectrometry (LC-MS/MS)-based metabolite profiling revealed 179 annotated metabolites that had significantly differential abundances between the studied bacterial strains and the control growth medium. Most of them belonged to classes such as amino acids and derivatives, organic acids, and nucleot(s)ides. Of particular interest, *Segatella copri* DSM 18205 (previously referred to as *Prevotella copri*) produced substantial quantities of the bioactive metabolites phenylethylamine, tyramine, tryptamine, and ornithine. *Parabacteroides merdae* CL03T12C32 stood out due to its ability to produce cadaverine, histamine, acetylputrescine, and deoxycarnitine. In addition, we found that strains of the genera *Bacteroides, Phocaeicola,* and *Parabacteroides* accumulated considerable amounts of proline-hydroxyproline, a collagen-derived bioactive dipeptide. Collectively, these findings offer a more detailed comprehension of the metabolic potential of these Bacteroidales strains, contributing to a better understanding of their role within the human gut microbiome in health and disease.

1. Introduction

The gastrointestinal tract harbors a diverse microbial community, primarily composed of bacteria, but also encompasses archaea, eukaryotes, and viruses (Backhed, 2005; Reyes et al., 2010). Within the host, this intricate assembly of microorganisms resembles a vital microbial organ (Backhed, 2005). It consumes, preserves, and redistributes energy; it carries physiologically relevant chemical transformations; and it restores itself through autonomous replication. As a consequence of all this metabolic activity, the gut microbiota is known to produce numerous metabolites, which can ultimately mediate microbe-host and microbe-microbe interactions (Donia and Fischbach, 2015). Furthermore, the microbiota's impact on the host is systemic, encompassing more than just the local effects in the gastrointestinal tract (Ahmed et al., 2022; Fernandez-Cantos et al., 2021; Liu et al., 2022; Zarei et al., 2022). Key communication networks that have garnered increasing attention include the gut-liver and the gut-brain axis, extensively reviewed elsewhere (Cryan et al., 2019; Tripathi et al., 2018), whose bidirectional communication is believed to govern numerous aspects of human health.

* Corresponding author.
E-mail address: o.p.kuipers@rug.nl (O.P. Kuipers).

https://doi.org/10.1016/j.micres.2024.127700
Received 15 December 2023; Received in revised form 5 March 2024; Accepted 18 March 2024
Available online 20 March 2024

The repertoire of metabolites isolated from intestinal microbes spans a wide array of chemical classes, including lipids, glycolipids, peptides, oligosaccharides, and amino acid derivatives (Donia and Fischbach, 2015). The origins are equally diverse, with some arising from the modification of host molecules, such as the secondary bile acid deoxycholic acid (DCA) (Yoshimoto et al., 2013). Others result from *de novo* biosynthesis, exemplified by antimicrobial peptides such as ABP-118 (Corr et al., 2007). Dietary precursors and medications also serve as valuable sources. For instance, intestinal microbes can metabolize essential amino acids, including phenylalanine, tryptophan, and lysine, yielding the bioactive products phenylethylamine, tryptamine, or cadaverine (Fernandez et al., 2001; Khan and Nawaz, 2016; Kovács et al., 2019; Miller, 2011). Additionally, medications can undergo transformation by the gut microbiota, as seen with the antidepressant derivative 5-hydroxyindole, a potent stimulant of intestinal motility (Waclawiková et al., 2021).

Among the inhabitants of the human gastrointestinal tract, Bacteroidales constitute the most abundant gram-negative order (Qin et al., 2010) and it exhibits remarkable stability (Faith et al., 2013). These obligate anaerobes have been the subject of extensive study due to their production of immunomodulatory molecules, their remarkable capacity to break down complex carbohydrates and fibers, and, more recently, their antimicrobial prowess. For instance, *Bacteroides fragilis* produces the immunomodulatory capsular polysaccharide A (PSA), which plays a vital role in bolstering the immune system and warding off bacterial and viral infections (Mazmanian et al., 2008; Ramakrishna et al., 2019; Round and Mazmanian, 2010). Production of antimicrobial molecules that mediate competition *in vivo* has been recently described for species of the genus *Bacteroides* (Roelofs et al., 2016). Moreover, Bacteroidales species have been implicated in the synthesis of neuroactive compounds, including short-chain fatty acids (SCFAs) and the neurotransmitter gamma-aminobutyric acid (GABA) (Gotoh et al., 2017; Horvath et al., 2022; Strandwitz et al., 2019). Yet, a comprehensive profile of compounds produced by Bacteroidales bacteria, including non-*Bacteroides* species, is lacking.

Liquid chromatography coupled with tandem mass spectrometry (LC-MS/MS), has become the prevailing choice for characterizing metabolic phenotypes, accommodating both targeted and non-targeted analyses (Gika et al., 2019; Johnson et al., 2016). Aiming to profile and identify as many metabolites as possible in a given biological sample, non-targeted metabolomics has shown its utility in identifying microbiome-derived metabolites as well as characterizing the host-microbiota interplay (Koistinen et al., 2019; Ni et al., 2023; Zarei et al., 2022). Here, we employed a non-targeted metabolomics approach to identify metabolites produced *in vitro* by six Bacteroidales strains. This investigation was conducted in modified Gifu anaerobic medium (mGAM) supplemented with mucin, a growth medium previously documented to resemble the gut microbiota's natural environment (Rettedal et al., 2014; Tramontano et al., 2018). Our selection encompassed representatives from the *Bacteroides* genus as well as strains from the genera *Phocaeicola, Parabacteroides,* and *Segatella* (Tramontano et al., 2018). We conducted statistical comparisons to pinpoint metabolites that had differences in abundance across Bacteroidales strains under the culture conditions tested, which led to the confident identification of 179 metabolites. Most of these metabolites belonged to classes such as amino acids and derivatives, nucleot(s)ides, and organic acids. Notably, *Segatella copri* DSM 18205 (previously referred to as *Prevotella copri*) and *Parabacteroides merdae* CL03T12C32 stood out for their capacity to produce bioactive amines, with the former accumulating phenylethylamine, tyramine, and tryptamine, and the latter cadaverine and histamine. In addition, we observed the accumulation of collagen-derived catabolites, namely proline-hydroxyproline, 4-hydroxyproline, and 5-hydroxylysine, in varying proportions among the Bacteroidales strains. Lastly, we further discuss for *S. copri* DSM 18205 and *Pa. merdae* CL03T12C32 other metabolites with a putative role in health and disease.

2. Materials and methods

2.1. Bacterial strains and growth conditions

All Bacteroidales strains used for this study are listed in Supplementary Table 1. Bacteroidales strains were grown in modified Gifu Anaerobic Medium (mGAM, HiFi Media, EWC Diagnostics) supplemented with porcine gastric mucin (M1778, Sigma-Aldrich). Mucin supplementation of mGAM was performed as described in Tramontano *et al.* (Tramontano et al., 2018): 20 g of porcine gastric mucin was dissolved per liter of phosphate saline buffer (PBS, pH 7.4), autoclaved at 121°C for 20 min and left standing overnight at room temperature. After centrifugation for 10 min at 7000 g, the supernatant was added to mGAM to a final concentration of 5 g/L. Bacteria were cultivated at 37°C under anaerobic conditions in a vinyl anaerobic chamber (COY Laboratory Products, Michigan, USA) inflated with a gas mix of approximately 5% CO_2 and 1.5–2% H_2.

2.2. Characterization of bacterial growth

Prior to the experiments, bacteria were streaked on mucin-containing mGAM agar plates and incubated for 24–48 h. Following this, liquid mGAM with mucin was inoculated with a single colony and incubated O/N under the same condition. This procedure was replicated three times for each bacterial strain. To monitor the bacterial growth profile, pre-cultures of each strain were centrifuged, washed with PBS, and inoculated into mGAM at an optical density of 0.0125 measured at 600 nm ($OD_{600\ nm}$). The growth was monitored in 0.2 mL cultures in 96-well micro-titer plates by using a microtiter plate reader Infinite F Nano+ (Tecan, Switzerland). Previously described anaerobic and temperature conditions were maintained throughout the growth curve assay. Every 15 min, after thorough orbital shaking at 159 rpm at an amplitude of 5 mm for 5 sec, growth was recorded by $OD_{600\ nm}$ measurements for up to 30 h. Raw growth curves were corrected for the background $OD_{600\ nm}$ of the mGAM supplemented with mucin broth and growth curve profiles were visualized using GraphPad Prism 8.0.2.

2.3. Non-targeted metabolite profiling analysis

2.3.1. Sample preparation

A total of five bacterial cell cultures per strain in the stationary phase (~18 h) were collected and the quenching metabolite extraction was adapted from Yuan *et al.* (Yuan et al., 2012). mGAM supplemented with mucin was used as control and processed in the same way as bacterial cell culture samples. Sample preparation was performed on dry ice to avoid the degradation of compounds. 700 μL of cooled aqueous HPLC grade methanol was added to 200 μL of cell culture. The resulting mixture was vortexed for 1 min and centrifuged at 14000 g for 10 min at 4°C. The supernatant was aliquoted and stored at −80℃ until further analysis. Prior to the analysis, all samples were diluted to obtain a final concentration of 80% v/v methanol and filtered (captiva ND filter plate 0.2 μm) by centrifuging at 14000 g for 10 min at 4℃ and kept at 4℃ until analysis. Quality control (QC) samples were prepared by aliquoting and pooling 2 μL of each analytical sample. Finally, solvent blank samples, constituted of 80% v/v aqueous HPLC grade methanol were included and processed in the same manner as the analytical samples.

2.3.2. LC-MS/MS analysis

Analysis of the samples using liquid chromatography tandem mass spectrometry (LC-MS/MS) for non-targeted metabolic profiling was performed according to Klåvus *et al.* (Klåvus et al., 2020).To obtain as maximum metabolite coverage as possible, two different chromatographic separation techniques were used, hydrophilic interaction (HILIC) and reversed-phase (RP) chromatographies. QC samples were injected at the beginning of the analysis and after every 9 analytical samples.

The LC-MS analysis was performed on a 1290 Infinity Binary UPLC coupled with a 6540 UHD Accurate-Mass quadrupole time-of-flight (QTOF) (Agilent Technologies Inc., CA, USA). For HILIC separation, Acquity UPLC BEH amide column (2.1×100 mm, 1.7 μm; Waters Corporation, Milford, MA) was used as the stationary phase with an injection volume of 3 μL. The temperature of the column was maintained at 45C and the mobile phase flow rate was 600 μL/min. The mobile phases were 50% v/v acetonitrile (eluent A) and 90% v/v acetonitrile (eluent B). Both eluents were supplemented with 20nmol/L ammonium formate, pH 3 (Sigma-Aldrich). The gradient elution was: 0–2.5 min, 100% B; 2.5–10 min, 100%B→0%B; 10–10.1 min, 0%B→100%B; 10.1–14 min, 100%B. For RP, Zorbax Eclipse XDB-C18 column (100 ×2.1 mm, 1.8 μm; Agilent Technologies Inc.) constituted the stationary phase. The temperature of the column was maintained at 50C and the mobile phase flow rate was 400 μL/min. The mobile phases were water (eluent A) and methanol (eluent B), both containing 0.1% v/v formic acid. The elution gradient was: 0–10 min, 2%B→100% B; 10–14.5 min, 100%B; 14.5–14.51 min, 100%B→2%B; 14.51–16.5 min, 2%B.

After each chromatographic separation, MS was equipped with heated electrospray ionization in both positive (ESI+) and negative (ESI-) modes. Collision energies for the MS/MS analysis were set at 10, 20, and 40 V for compatibility with spectral databases (Kim et al., 2016; Smith et al., 2005; Wishart et al., 2007). MassHunter Acquisition 10.0 software (Agilent Technologies Inc.) was used for data acquisition.

2.3.3. Data analysis

Raw instrumental data (*.d files) was converted into Abf format using Reifycs Abf Converter (https://www.reifycs.com/AbfConverter). Subsequently, peak picking and alignment were performed according to Klåvus *et al.* (Klåvus et al., 2020). Briefly, automated peak picking and alignment were performed using MS-DIAL (version 4.9) (Tsugawa et al., 2015). The minimum peak height was set to 2000, MS/MS tolerance to 0.05, and retention time (RT) tolerance to 0.1 min. Default settings were used for the remaining parameters. After peak picking, the alignment result as peak areas was exported into a Microsoft Excel datasheet. The resulting four datasheets, one for each chromatographic separation technique and ionization mode, were combined into a single file. Then, signals detected in less than 70% of the pooled QC samples were not included for further data analysis. Drift correction was applied according to Klåvus *et al.* (Klåvus et al., 2020) in order to correct for the systematic intensity drift induced by the LC-MS analytical sequence. After drift correction, features with an RSD*<0.2 and D-ratio*<0.4 or RSD*<0.1, RSD <0.1 and D-ratio<0.1 were retained (Klåvus et al., 2020).

All statistical analyses were conducted using R package (4.1.1). One-way ANOVA was performed to detect differentially abundant molecular features. Subsequently, to detect metabolites at significantly higher or lower levels in each bacterial culture compared to the control media, Welsch's t-test was applied. Both one-way ANOVA and t-test *p*-values were adjusted for multiple comparisons using the Benjamini-Hochberg false-discovery rate method (FDR). Only statistically significant features ($p<0.05$) with MS/MS spectra and with an arbitrary value for the average peak area of at least 10,000 were annotated. Annotation was performed using MS-DIAL (version 4.9) (Tsugawa et al., 2015). The exact *m/z*, RT, and MS/MS fragmentation patterns of each signal were compared against our in-house standard library and publicly available spectral databases, such as METLIN (https://metlin.scripps.edu), MassBank of North America (https://mona.fiehnlab.ucdavis.edu), and Human Metabolome Database (HMDB, www.hmdb.ca). MS-FINDER (version 3.52) (Tsugawa et al., 2016) and METLIN (Guijas et al., 2018) were used to characterize the unknowns, those signals for which no exact match was available in our in-house library nor public databases. Agilent MassHunter Qualitative Analysis 10.0 was used to explore raw data extracted ion chromatograms (EICs) and MS/MS fragmentation data. Annotated metabolites were classified into one of the four identification levels based on criteria established by Summer et al. (Sumner et al., 2007). Level 1 signified identified metabolites using a chemical reference standard, level 2 designates putatively annotated compounds relying on public spectral libraries, level 3 denotes putatively characterized compound classes, and level 4 signifies unknown compounds. Levels 1 and 2 are regarded as annotations with a high degree of confidence.

Following metabolite identification, principal component analysis (PCA) was applied to good-quality molecular features (n=11,105). Fold change values (FC) for each identified metabolite were calculated for each Bacteroidales strain by dividing its average signal abundance by that of the control media samples. Afterward, the top 25 most significantly increased metabolites on each Bacteroidales strain were selected based on a $\log_2 FC>0$ and the highest significance ($-\log_{10} q$ value). Data representation via PCA, heatmap, and bar charts was performed using an in-house custom script based on ggplot2 packages in R (version 4.3.1). Adobe Illustrator 2023 was used for figure composition and Chemdraw v22.2.0 for chemical structure representation. Heatmap representation of $\log_2 FC$ values for each sample type applying unsupervised hierarchical clustering to both bacterial samples and identified metabolites was generated using ClustVis (Metsalu and Vilo, 2015).

2.4. Metabolic pathway analysis and genome mining

Metabolic pathway analysis of the metabolites discussed was conducted using MetaboAnalyst 5.0 (Pang et al., 2022) and the Kyoto Encyclopedia of Genes and Genomes (KEGG) database (https://www.genome.jp/kegg/) (Kanehisa and Goto, 2000). Initially, the metabolite's HMDB IDs were used as input in MetaboAnalyst 5.0 for pathway analysis, yielding KEGG pathway map IDs. Subsequently, KEGG maps and compound IDs were used as input in the KEGG database, facilitating the identification of the enzymes involved in the specific metabolic pathway under investigation. The enzyme commission numbers (ECs) associated with these enzymes were then extracted and used for genome mining purposes. The ECs and the enzyme names served as input into the National Center for Biotechnology Information (NCBI) protein database (https://www.ncbi.nlm.nih.gov/protein), applying tailored filters to narrow down the search to the genomes of the bacterial strains used in this study.

3. Results and discussion

3.1. Selection of representative gut Bacteroidales strains and growth profile determination

To study the metabolome of gut commensal Bacteroidales bacteria, we selected six bacterial strains representing three different and relevant families within the order Bacteroidales: *Bacteroidaceae*, *Prevotellaceae*, and *Tannerellaceae*. Notably, five of these six strains are part of the core species within the human gut microbiota according to Tramontano *et al.* (Tramontano et al., 2018). These strains are *Bacteroides fragilis* NCTC 9343, *Bacteroides stercoris* DSM 19555, *Phocaeicola dorei* CL02T12C06 (previously known as *Bacteroides dorei* CL02T12C06), *Parabacteroides merdae* CL03T12C32, and *Segatella copri* DSM 18205 (previously designated as *Prevotella copri* DSM 18205). In addition to these well-established species, we also included the unclassified *Bacteroides* sp. 4 1 36 due to its promising potential as a next-generation probiotic (Garcia-Morena et al., 2024). To simulate *in vitro* their natural environment, the strains were cultivated in modified Gifu anaerobic medium (mGAM) broth, a growth media previously documented to simulate the gut microbiota's natural environment (Rettedal et al., 2014; Tramontano et al., 2018). Furthermore, mucin was added to the mGAM broth (see Methods) due to its growth-promoting capabilities (Tramontano et al., 2018).

Due to the lack of growth phase determination of gut commensals *in vivo* and the interpersonal variability described in metagenomic samples (Korem et al., 2015; Lim et al., 2023), we prioritized measuring the

metabolite profile in the stationary phase. This approach guarantees sufficient accumulation of metabolites and fosters consistency in experimental conditions across replicates and bacterial strains. To determine the optimal sampling time-point at which the six strains had entered the stationary phase, their growth in mGAM supplemented with mucin was monitored by measuring the optical density at 600 nm ($OD_{600\ nm}$) under anaerobic conditions (Supplementary Figure 1). After 18 hours of incubation, all six bacterial strains had reached the stationary phase and, hence, we selected this incubation time to profile their metabolome.

3.2. Non-targeted LC-MS/MS metabolomics analysis of Bacteroidales strains in stationary phase reveals distinctive metabolite profiles

High resolution LC-MS/MS in four analytical modes, RP and HILIC modes with both positive and negative ionization, detected a total of 11,105 good-quality features across samples. Overall differences in metabolite composition among samples were visualized via a principal component analysis (PCA), performed using these molecular features (Fig. 1). The metabolite composition of *B. fragilis* NCTC 9343, *Bacteroides* sp. 4 1 36, *Ph. dorei* CL02T12C06, and *Pa. merdae* CL03T12C21 DSM 19555 cell cultures were the most similar to each other. *B. stercoris* DSM 19555 and *S. copri* DSM 18205 presented distinctive metabolite compositions. Notably, *S. copri* DSM 18205 showed a metabolite profile more similar to the uncultivated mGAM supplemented with mucin than to the rest of the Bacteroidales strains. Next, features exhibiting significant changes in abundance across samples were identified, yielding a total of 613 features. Among these, we annotated 179 metabolites with a high level of confidence (Supplementary Table 2). Most of them belonged to classes such as amino acids and derivatives, nucleot(s)ides, and organic acids. The heatmap representation of these confidently annotated metabolites, applying unsupervised clustering (Supplementary Figure 2), further confirmed the similarity in the metabolomes of *B. fragilis* NCTC 9343, *Bacteroides* sp. 4 1 36, and *Ph. dorei* CL02T12C06. In accordance with the PCA, *S. copri* DSM 18205 showed the most distinctive profile, positioning it as the outermost branch of the clustering tree. The variations in metabolite profiles we observed are not in sync with the phylogenetic classification of these bacterial strains by family (García-López et al., 2019). Although *Bacteroidaceae* and *Prevotellaceae* families share a closer phylogenetic relationship, *S. copri* DSM 18205 displayed significant differences in its metabolomic profile compared to *Bacteroides* and *Phocaeicola* strains. In contrast, *Pa. merdae* CL03T12C32, belonging to the more distant *Tannerellaceae* family, exhibited greater similarities to the *Bacteroidaceae* strains.

We further selected and discussed the top 25 most significantly increased metabolites within each bacterial cell culture in order to highlight relevant metabolites that these bacteria can produce. This yielded a total of 61 distinct metabolites after considering overlaps across strains. Our findings revealed that the predominant category of compounds exhibiting substantial increases consisted of amino acids and derivatives (Fig. 2). This category includes peptides, amino acids, amines, and other metabolites of amino acids. Within peptides, proline-hydroxyproline was notably accumulated in significant quantities. Additionally, other peptides accumulated include aspartyl-arginine and Gly-Val-Arg. Several amino acids demonstrated an increased abundance, with *S. copri* DSM 18205 accumulating particularly high levels of ornithine. Amines were predominantly found in *S. copri* DSM 18205 and *Pa. merdae* CL03T12C32 cell cultures. *S. copri* accumulated tyramine, tryptamine, and phenylethylamine, while *Pa. merdae* showed a significant accumulation of histamine, cadaverine, agmatine, and acetylputrescine. Other bacterial strains also accumulated relevant amounts of agmatine such as *B. stercoris* DSM 19555 and *Ph. dorei* CL02T12C06. Other increased amino acid derivatives include urocanic acid, citrulline, 5-hydroxylysine, and 4-hydroxyproline. Nucleot(s)ides was the second group with the most metabolites significantly increased. Metabolites identified under this class are purine and pyrimidine metabolites which serve as building blocks for DNA and RNA and provide a cell with sufficient energy and cofactors for cell survival and proliferation (Pedley and Benkovic, 2017). The third most prominent class is organic acids derived from energy metabolism. *S. copri* DSM 18205 accumulated significant amounts of 2-hydroxybutanoic acid and lactic acid. *Bacteroides* sp. 4 1 36 produced lactic acid in remarkable quantities as well. Aconitate and malic acid were found in significant amounts by *B. stercoris* DSM 19555, *Bacteroides* sp. 4 1 36, *B. fragilis* NCTC 9343, and *Ph. dorei* CL02T12C06. Notably, the abundance of aconitate and malic acid in *Ph. dorei* CL02T12C06 cell culture was approximately 20 and 16 times higher than in the control, respectively. *Pa. merdae* CL03T12C32 was the only strain exhibiting substantial accumulation of deoxycarnitine, a straight-chain fatty acid.

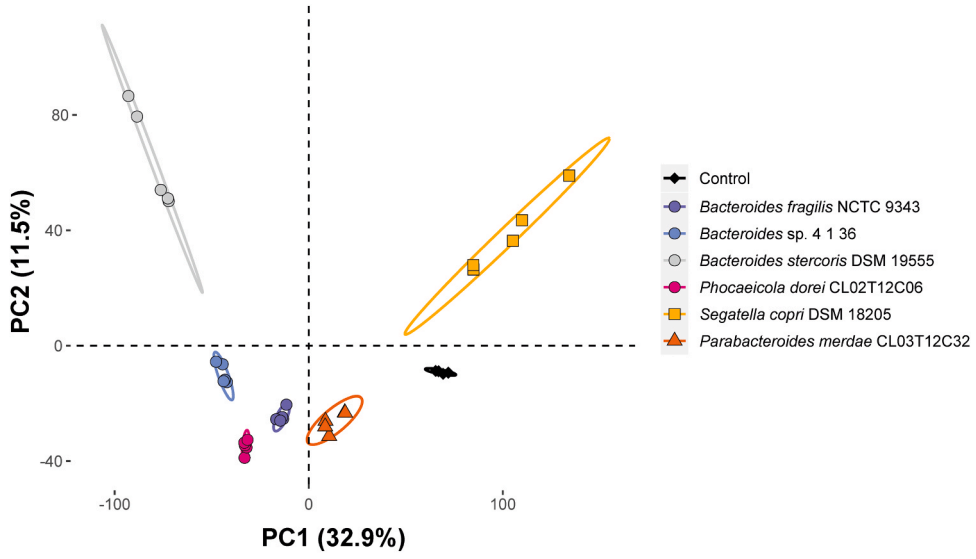

Fig. 1. Principal component analysis (PCA) derived from non-targeted metabolomic data of Bacteroidales cell cultures in the stationary phase. The dataset includes all molecular features (n=11,105) detected across the four analytical modes. The two principal components are shown, which explain 32.9% and 11,5% of the variation within the data, respectively. Ellipses were drawn for each sample type with a 90% level of confidence. Spherical, squared, and triangular points represent bacteria from the *Bacteroidaceae*, *Prevotellaceae*, and *Tannerellaceae* families, respectively.

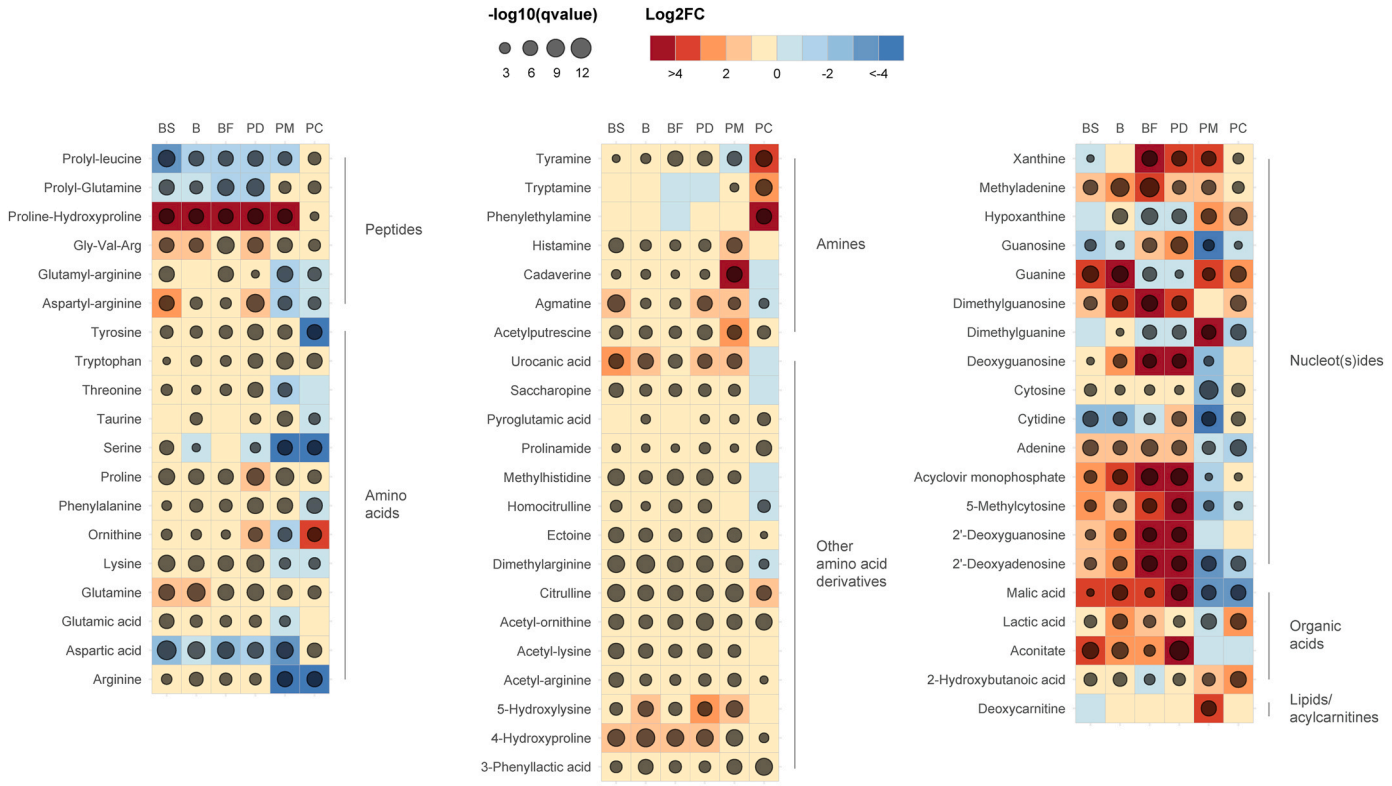

Fig. 2. Heatmap representation of the top 25 significantly increased metabolites on at least one Bacteroidales cell culture. Fold-change (FC) and degree of significance comparisons (t-test and Benjamini-Hochberg false discovery rate correction p value<.05 and q value<.05) were calculated between each bacterial cell culture and control media. Red and blue cells represent metabolites with increased and decreased abundance, respectively. The degree of significance is represented with a circle inversely proportional to the q value. BS: *Bacteroides stercoris* DSM 19555, B: *Bacteroides* sp. 4 1 36, BF: *Bacteroides fragilis* NCTC 9343, PD: *Phocaeicola dorei* CL02T12C06, PM: *Parabacteroides merdae* CL03T12C32, and SC: *Segatella copri* DSM 18205.

3.3. Bacteroidales production of biogenic amines resulting from amino acid decarboxylation

Several decarboxylation products of proteinogenic L-amino acids (Fig. 3) were detected during our analysis. Decarboxylation of L-amino acids has previously been shown as a strategy in certain bacteria to adapt to acidic environmental conditions (Schwarz et al., 2022). The dedicated decarboxylase consumes a H^+ while converting the specific amino acid into a more alkaline product, which is then exported by a specific antiporter in exchange for the amino acid (Connil et al., 2002; Han and Shin, 2022; Hersh et al., 1996; Iyer et al., 2003; Pereira et al., 2009; Schwarz et al., 2022; Wolken et al., 2006). The accumulation of different organic acids (Fig. 2) as a result of energy metabolism provides support for media acidification. Moreover, it is worth noting that Bacteroidales are known producers of short-chain fatty acids (SCFAs) (Gotoh et al., 2017; Horvath et al., 2022; Zafar and Saier, 2021), metabolites known to acidify the environment, but which are not detected by LC-MS methodology. This strengthens the hypothesis that the decarboxylation of L-amino acids is an adaptive mechanism in response to acidic environments. As colonizers of the human gastrointestinal tract and one of its most prevalent members (Qin et al., 2010; Tramontano et al., 2018), Bacteroidales bacteria must endure varying pH conditions, including the low pH in the stomach and the slightly acidic environment of the colon (Schwarz et al., 2022). The decarboxylation of amino acids likely serves as an adaptive mechanism under these conditions and we hypothesize that the resulting alkaline products are exported to the extracellular medium as previously shown for other bacteria (Connil et al., 2002; Han and Shin, 2022; Hersh et al., 1996; Iyer et al., 2003; Pereira et al., 2009; Schwarz et al., 2022; Wolken et al., 2006). It is worth noting that the tested bacteria showed distinct preferences on this property. Mainly, *S. copri* DSM 18205 decarboxylated aromatic L-amino acids (Fig. 3A-**C**) and *Pa. merdae* CL03T12C32 did so with positively charged L-amino acids (Fig. 3D**&E**). All Bacteroidales strains except for *S. copri* also decarboxylate arginine, producing agmatine (Fig. 3F).

Notably, compared to the control, *S. copri* DSM 18205 accumulated around 50 and 10 times higher levels of phenylethylamine and tyramine, respectively (Fig. 3A**&B**). Phenylethylamine, tyramine, and tryptamine result from the enzymatic decarboxylation of the aromatic amino acids phenylalanine, tyrosine, and tryptophan respectively (KEGG pathways map00360, map00350, and map00380). These reactions are carried out by aromatic L-amino acid decarboxylases (AADCs) (Schwarz et al., 2022). To date, several bacterial AADCs have been identified in different microorganisms, showing different substrate specificity (Choi et al., 2021; Kezmarsky et al., 2005; Moreno-Arribas and Lonvaud-Funel, 2001; Perez et al., 2015; van Kessel et al., 2019; Williams et al., 2014). To identify whether *S. copri* DSM 18205 encodes any AADC, its genome was screened for tyrosine decarboxylase (EC 4.1.1.25), aromatic-L-amino-acid decarboxylase (EC 4.1.1.28), tryptophan decarboxylase (EC 4.1.1.105), and phenylalanine decarboxylase (EC 4.1.1.53). No putative enzyme with a similar function was detected.

The substantial accumulation of the biogenic amines phenylethylamine, tyramine, and tryptamine by *S. copri* DSM 18205 could hold local and systemic implications if produced in the gastrointestinal tract. Commonly referred to as trace amines (TAs) due to their low concentration in the central nervous system (Berry, 2004), they act as neurotransmitters or neuromodulators (Khan and Nawaz, 2016; Miller, 2011). Phenylethylamine, which has been shown to be able to cross the blood-brain barrier, is a dopamine receptor agonist (Chen et al., 2019). Tryptamine is a monoamine similar to serotonin that is able to bind the serotonin 5-HT_4 receptor in the colonic epithelium increasing colonic secretion and, hence, gastrointestinal transit (Bhattarai et al., 2018). Tyramine has been shown to stimulate host production of serotonin both

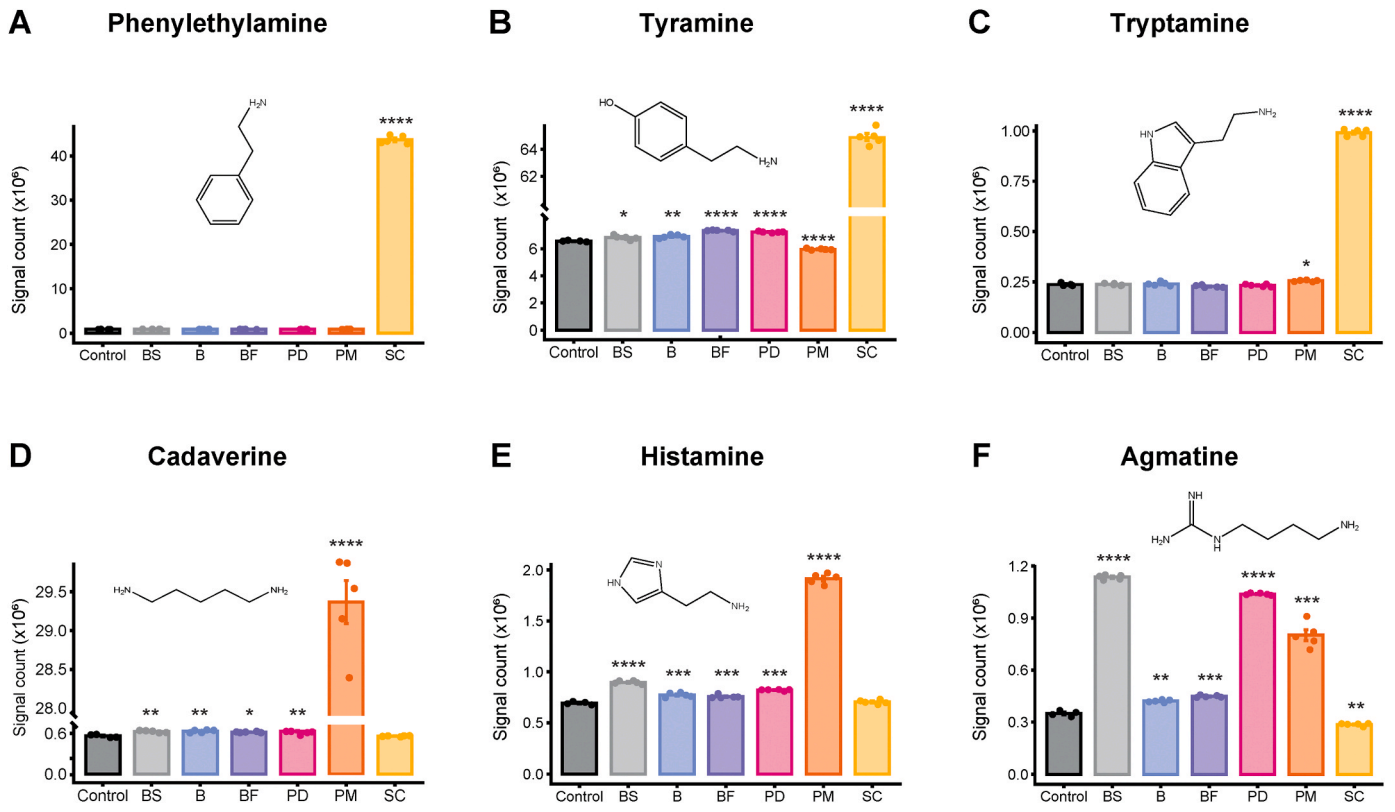

Fig. 3. Biogenic amines product of amino acid decarboxylation: phenylethylamine (A), tyramine (B), tryptamine (C), cadaverine (D), histamine (E), and agmatine (F). Statistical significance between each bacterial cell culture and the control is shown using asterisks (* q<0.05, ** q<0.01,*** q<0.001, **** q<0.0001). Bars represent the average signal count of each strain, error bars denote standard deviation (SD), and individual dots represent the signal count of each replicate. BS: *Bacteroides stercoris* DSM 19555, B: *Bacteroides* sp. 4 1 36, BF: *Bacteroides fragilis* NCTC 9343, PD: *Phocaeicola dorei* CL02T12C06, PM: *Parabacteroides merdae* CL03T12C32, and SC: *Segatella copri* DSM 18205.

in vivo and *in vitro* (5-HT), a neurotransmitter and an important factor in the gastrointestinal tract and other organs (Yano et al., 2015). Moreover, tyramine accumulation by this strain could be relevant not only for the physiological implications of this biogenic amine. The elegant study of van Kessel *et al.* showed concomitant decarboxylation of tyrosine and levodopa by tyrosine decarboxylases from *Lactobacillus* spp. and *Enterococcus* spp. This holds special relevance for Parkinson's disease treatment, where levodopa is used as a primary treatment to increase dopamine concentrations. The authors showed that a higher abundance of tyrosine decarboxylase genes in the jejunum negatively correlates with levodopa levels in plasma (van Kessel et al., 2019). We could not identify any tyrosine decarboxylase in the genome of *S. copri* DSM 18205 based on homology to previously described enzymes. We hypothesize that a non-orthologous enzyme is carrying the reaction, suggesting new roles of this bacterial strain in health and disease.

Moreover, phenylethylamine and tryptamine have recently been shown to impair insulin sensitivity in irritable bowel disease and metabolic syndrome (Zhai et al., 2023). The link of *S. copri* DSM 18205 to inflammatory diseases and insulin resistance has been previously reported. Pedersen *et al.* identified *S. copri* DSM 18205 as one of the main species driving the association between insulin resistance and biosynthesis of branched chain fatty acids (BCAAs). It is important to note that the study of the effect of *S. copri* DSM 18205 on the host metabolome was reduced to a subset of metabolites previously correlated to a population of Danish individuals (Pedersen et al., 2016). Unfortunately, this subset did not include phenylethylamine or tryptamine and, hence, it cannot be excluded a possible association between the production of these biogenic amines by *S. copri* DSM 18205 and insulin resistance.

Pa. merdae CL03T12C32 exhibited significant accumulation of cadaverine and histamine, products of decarboxylation of lysine and histidine respectively (KEGG pathway map00310 and map00340; Fig. 3D&E). It is noteworthy that the abundance of cadaverine in the *Pa. merdae* CL03T12C32 cell culture was 60 times higher than in the control. Even though cadaverine has been frequently associated with periodontal disease (Levine and Lohinai, 2021), this biogenic amine has also been linked to inhibition of breast cancer growth (Kovács et al., 2019) and bacterial virulence inhibition (Fernandez et al., 2001; McCormick et al., 1999). Interestingly, *Pa. merdae* showed a lower abundance in breast cancer patients compared to healthy controls (Shrode et al., 2023). Shrode *et al.* mainly focused on the reduction of SCFA-producing bacteria in breast cancer patients as a causative effect. However, in light of the effect of cadaverine as a reductor of breast cancer aggressiveness through trace amino acid receptors (TAARs) (Kovács et al., 2019), the role of reduced *Pa. merdae* and, hence, cadaverine production in the pathobiology of breast cancer cannot be excluded. Histamine also plays diverse and essential roles in human physiology, acting as a neurotransmitter, simulating gastric secretion, or as part of the immune response to allergens and pathogens (Fiorani et al., 2023; Parsons and Ganellin, 2006). Lysine decarboxylase (EC 4.1.1.18) and histidine decarboxylase (EC 4.1.1.22) are the enzymes catalyzing these reactions. Genome mining of *Pa. merdae* CL03T12C32 did not reveal any putative enzymes responsible for these functions.

Finally, all Bacteroidales cultures, except for *S. copri* DSM 18205, accumulated significant amounts of agmatine, the decarboxylation product of arginine (KEGG pathway map00330, Fig. 3F). In a study by Haenisch *et al.*, it was noted that *Phocaeicola vulgatus* DSM 1447, a closely related bacterial strain to *Ph. dorei* CL02T12C06, exhibited significant agmatine production. Consistent with our findings, the authors showed that *B. fragilis* NCTC 9343 produces agmatine at comparatively lower concentrations than *Ph. vulgatus* DSM 1447 (Haenisch et al.,

2008). The production of agmatine by these Bacteroidales strains holds significance to the influence of this amine in gut motility, the secretion of digestive enzymes, and its positive effects on gut integrity, as well as its role in regulating glucose and fatty acid metabolism and insulin signaling (Nissim et al., 2014; Ramos-Molina et al., 2019; Saha et al., 2023). Additionally, microbiota-derived agmatine has been proposed to be absorbed from the lumen into the bloodstream via the action of specific transport mechanisms in enterocytes (Ramos-Molina et al., 2019). The presence of agmatine in systemic circulation has been suggested to exert favorable neuromodulatory effects (Saha et al., 2023). Arginine decarboxylase is a common trait in all the bacterial strains tested (EC 4.1.1.19, Supplementary Table 3).

3.4. Collagen-related catabolites are accumulated on Bacteroidales cell cultures

Collagen is the most abundant structural protein in animals and 28 different types of collagens have been described (Shoulders and Raines, 2009). They share a structural motif in which a trio of parallel polypeptide strands, arranged in a left-handed, polyproline II-type (PPII) conformation, coil about each other forming a right-handed triple helix, characterized by a one-residue stagger (Shoulders and Raines, 2009). The packing of the PPII helices presents a repeating XaaYaaGly peptide sequence, in which Xaa and Yaa can be any amino acid. However, the most frequently found amino acids in these positions are proline (Pro, 28%) and 4-hydroxyproline (Hyp, 38%), respectively. In addition, the most common triplet is Pro-Hyp-Gly with a 10.5% (Ramshaw et al., 1998). All Bacteroidales strains exhibited accumulation of the dipeptide proline-hydroxyproline (Pro-Hyp), in varying proportions depending on the strain (Fig. 4**A**). This suggests cleavage of the collagen triplet between the 4-hydroxyproline and glycine residues. The presence of collagen and collagen-like proteins in the growth media can be attributed to the composition of the mGAM medium, which includes extracts from various animal products (Gotoh et al., 2017). Microbial collagenases (EC 3.4.24.3) are enzymes described for their ability to degrade collagens in their triple helical regions at X-Gly bonds (Bhagwat and Dandge, 2018). Described microbial collagenases include metalloproteases (M9 family), serine proteases (S1, S8, and S53 families), and some members of the peptidase U32 family (Bhagwat and Dandge, 2018). *B. fragilis* NCTC 9343, *Pa. merdae* CL03T12C32, *S. copri* DSM 18205, and *B. stercoris* DSM 19555 encode putative collagenases (Supplementary Table 3). These collagenases exhibit similarities to enzymes belonging to the U32 family, specifically PrtC, which is found in the periodontal pathogen *Porphyromonas gingivalis* (Takahashi et al., 1991). However, *Bacteroides* sp. 4 1 36 and *Ph. dorei* CL02T12C06 do not present any putative collagenase in their genomes, despite the significant accumulation of collagen-derived metabolites in their bacterial cell cultures. This suggests the potential existence of non-orthologous collagenases or the possibility that these metabolites originate from other proteins distinct from collagen.

Two other collagen-related metabolites were detected in our study. 4-hydroxyproline was significantly accumulated in every bacterial cell culture (Fig. 4**B**). This metabolite mainly exists in collagen and, in mammalian systems, prolyl hydroxylases post-translationally hydroxylate L-proline residues to 4-hydroxyproline in procollagen (Zhang et al., 2021). Nevertheless, microbial hydroxylation of free L-proline to 4-hydroxyproline via proline 4-hydroxylases (EC 1.14.11.57) has been detected for a few bacterial species (Shibasaki et al., 1999). The genomes of the bacterial strains used in our study were screened for the presence of proline 4-hydroxylase genes, but no putative gene was identified. The last collagen-related metabolite is 5-hydroxylysine, which was significantly increased in all bacterial cell cultures, except for *S. copri* DSM 18205 (Fig. 4**C**). 5-hydroxylysine is also produced by the post-translational hydroxylation of lysine by lysine hydroxylases (EC 1.14.11.4) (Yamauchi and Shiiba, 2008). No lysine hydroxylase was detected in the genome of the screened strains.

Collagenase activity in microorganisms has been usually linked to pathogenicity (Bhagwat and Dandge, 2018). While Bacteroidales species are recognized as beneficial members of the human gut microbiota, *Bacteroides* spp. can become opportunistic pathogens, often contributing to polymicrobial infections at various body sites (Wexler, 2007; Zafar and Saier, 2021). This collagenase activity may help these bacteria in compromising the integrity of tissue barriers allowing them to access deeper tissues. Furthermore, the presence of collagenolytic bacteria in the gastrointestinal tract is of relevance, given their newfound association with the progression of colon cancer and the occurrence of post-surgical tumor growth (Gaines et al., 2020; Williamson et al., 2022).

3.5. Other metabolites

Gut Bacteroidales strains also accumulated significant amounts of ornithine, the polyamine acetyl-putrescine, and the straight-chain fatty acid deoxycarnitine (Fig. 5). *S. copri* DSM 18205 produced 10 times higher amounts of ornithine compared to the control (Fig. 5 **A**). This non-proteinogenic amino acid can be biosynthesized from arginine, proline, or glutamate (KEGG pathway map00330). Recently, the importance of ornithine in maintaining a healthy gut mucosa was demonstrated in lactobacilli (Qi et al., 2019). Qi *et al.* showed that lactobacilli-derived ornithine can upregulate L-kynurenine in gut

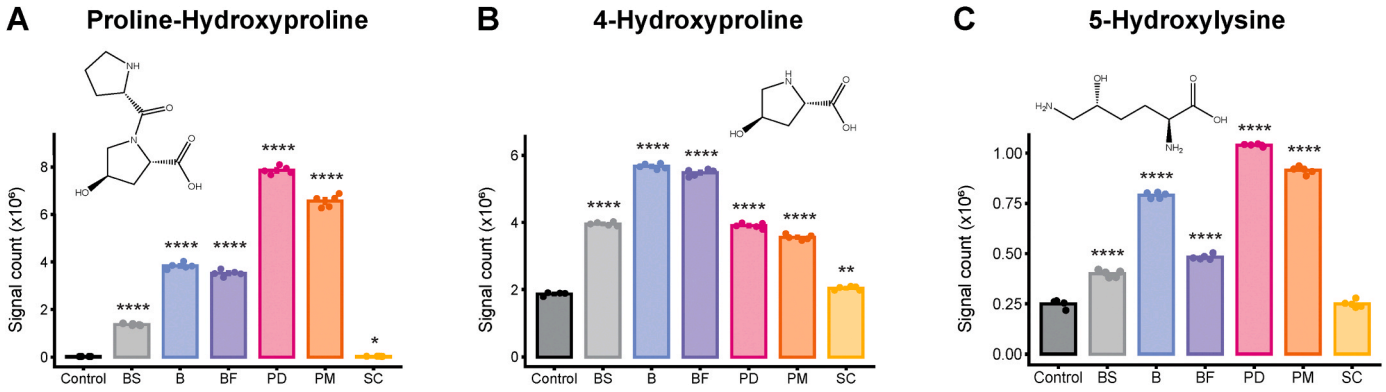

Fig. 4. Collagen-derived metabolites on each bacterial cell culture. This includes proline-hydroxyproline (A), 4-hydroxyproline (B) and 5-hydroxylysine (C). Statistical significance between each bacterial cell culture and the control is shown using asterisks (* q<0.05, ** q<0.01,*** q<0.001, **** q<0.0001). Bars represent the average signal count of each strain, error bars denote SD, and individual dots represent the signal count of each replicate. BS: *Bacteroides stercoris* DSM 19555, B: *Bacteroides* sp. 4 1 36, BF: *Bacteroides fragilis* NCTC 9343, PD: *Phocaeicola dorei* CL02T12C06, PM: *Parabacteroides merdae* CL03T12C32, and SC: *Segatella copri* DSM 18205.

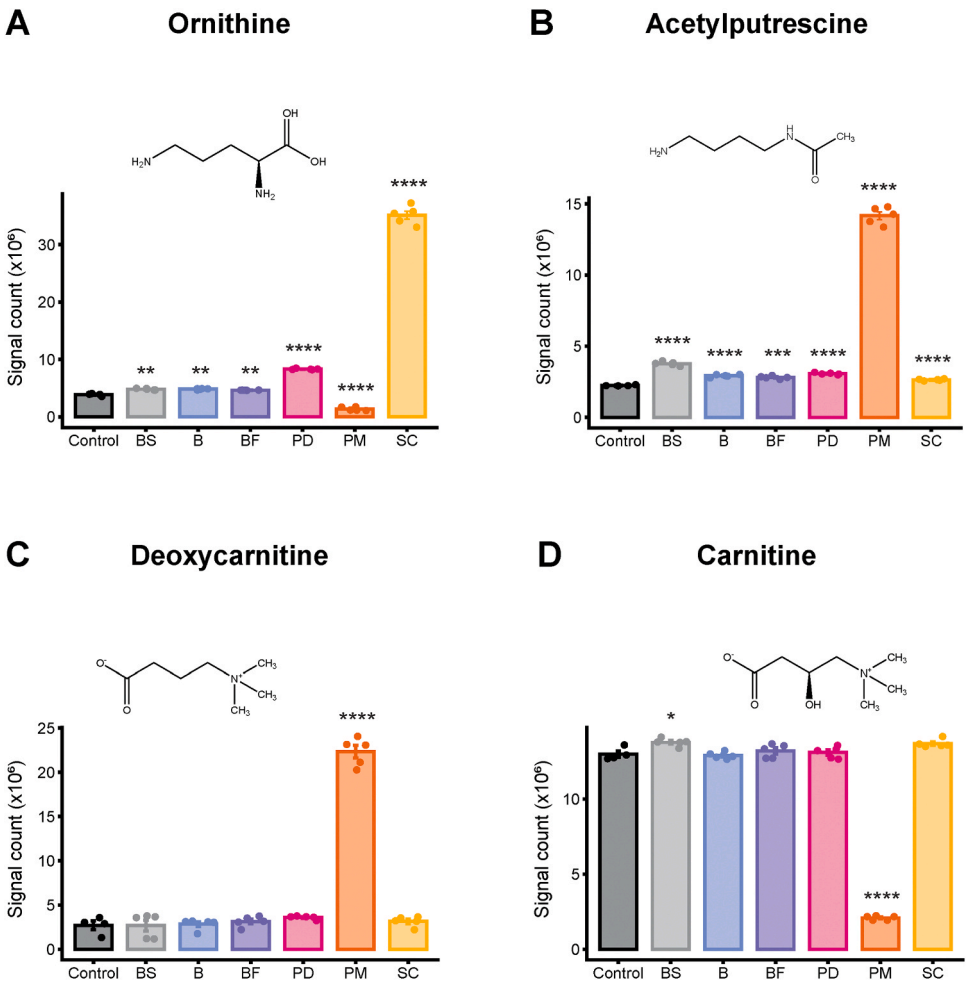

Fig. 5. Other metabolites differentially accumulated in Bacteroidales cell cultures: ornithine (A), acetylputrescine (B), deoxycarnitine (C), and carnitine (D). Statistical significance between each bacterial cell culture and the control is shown using asterisks (* q<0.05, ** q<0.01,*** q<0.001, **** q<0.0001). Bars represent the average signal count of each strain, error bars denote SD, and individual dots represent the signal count of each replicate. BS: *Bacteroides stercoris* DSM 19555, B: *Bacteroides* sp. 4 1 36, BF: *Bacteroides fragilis* NCTC 9343, PD: *Phocaeicola dorei* CL02T12C06, PM: *Parabacteroides merdae* CL03T12C32, and SC: *Segatella copri* DSM 18205.

epithelial cells, influencing the proliferation of mucosal cells and mucin production. Additionally, acetylputrescine, the N-acetylated form of putrescine, was significantly accumulated in all bacterial cell cultures. It was 6 times more abundant in *Pa. merdae* CL03T12C32 cell culture compared to the control (Fig. 5**B**). Biosynthesis of putrescine can be achieved via ornithine, agmatine or spermidine (KEGG pathway map00330). Its N-acetylated form, acetyl putrescine, is the first intermediary in the biosynthesis of the primary inhibitory neurotransmitter GABA. Nevertheless, no significant amounts of GABA were found to be accumulated on any strain. Interestingly, Strandwitz *et al.* found that *Bacteroides* spp. and *Parabacteroides* spp. actively express GABA-producing pathways in healthy individuals. This study pointed to the *B. fragilis* KLE1758 as a GABA producer via decarboxylation of glutamate induced at a low pH (pH<5.5). In contrast, as mentioned earlier, our *B. fragilis* NCTC 9343 did not accumulate this inhibitory neurotransmitter. This could be explained by the fact that the production of GABA by *B. fragilis* KLE1758 appears to be primarily observed when the bacterium is cultured on Petri dishes, where it acidifies the medium sufficiently to produce GABA (Strandwitz et al., 2019). Finally, *Pa. merdae* CL03T12C32 produced significant amounts of deoxycarnitine (Fig. 5 **C**). Bacteria living in anaerobic environments, where oxygen does not serve as a final electron acceptor, use alternative electron acceptors. L-carnitine can serve this purpose for some anaerobes (Meadows and Wargo, 2015; Seim et al., 1982). Even though crotonic acid betaine was not detected in our analysis, a significant consumption of carnitine was registered for *Pa. merdae* CL03T12C32 (Fig. 5**D**), supporting its use of carnitine as an electron acceptor. Although the precise mechanistic details remain unclear, deoxycarnitine has shown to have a positive association with gut permeability in cases of environmental enteric dysfunction (Semba et al., 2017).

4. Conclusions

A diverse collection of metabolites has been isolated from cultures of human-associated bacteria, some of which are well-documented as key players in the interactions between microbes and their hosts, as well as in inter-microbial communication. The present study thoroughly characterizes the *in vitro* metabolite profiles of six Bacteroidales strains cultivated until the stationary phase on mGAM supplemented with mucin. This comprehensive analysis enhances our understanding of their metabolic capabilities, uncovering multiple bioactive metabolites previously unassociated with them. Our findings showed that *S. copri* DSM 18205 accumulated considerable amounts of various bioactive metabolites, including phenylethylamine, tyramine, tryptamine, and ornithine. Noteworthy was also the ability of *Pa. merdae* CL03T12C32 to produce other bioactive metabolites, such as cadaverine, histamine, acetylputrescine, and deoxycarnitine. Furthermore, our research revealed the accumulation of substantial quantities of collagen-derived

metabolites, particularly the dipeptide proline-hydroxyproline, mainly in strains of *Bacteroides, Phocaeicola,* and *Parabacteroides.* The common absence of identifiable enzymatic candidates crucial for the biosynthesis of these molecules, position these strains as promising prospects for novel enzyme discovery. In addition, future research will be critical to determine the actual *in vivo* production of these metabolites and, should it be established, to unravel its implications for host physiology.

Funding

This work was supported by the ITN Marie Curie BestTreat-Building a Gut Microbiome Engineering Toolbox for In Situ Therapeutic Treatments for Non-alcoholic Fatty Liver Disease (grant number 813781). K. H. is supported by Research Council of Finland (grant no. 321716) and ERA-NET NEURON (grant no. 334814).

CRediT authorship contribution statement

Kati Hanhineva: Writing – review & editing, Supervision, Resources. **Ambrin Farizah Babu:** Writing – review & editing, Validation, Investigation, Formal analysis. **Maria Victoria Fernandez-Cantos:** Writing – review & editing, Writing – original draft, Visualization, Validation, Investigation, Conceptualization. **Oscar P. kuipers:** Writing – review & editing, Supervision, Resources.

Declaration of Competing Interest

The authors declare that they have no known competing financial interests or personal relationships that could have appeared to influence the work reported in this paper.

Data Availability

Data will be made available on request.

Acknowledgements

The authors acknowledge BEI Resources, NIAID, and NIH for providing some the bacterial strains used in this study.

Appendix A. Supporting information

Supplementary data associated with this article can be found in the online version at doi:10.1016/j.micres.2024.127700.

References

Ahmed, H., Leyrolle, Q., Koistinen, V., Kärkkäinen, O., Layé, S., Delzenne, N., Hanhineva, K., 2022. Microbiota-derived metabolites as drivers of gut–brain communication. Gut Microbes 14, 2102878. https://doi.org/10.1080/19490976.2022.2102878.

Backhed, F., 2005. Host-bacterial mutualism in the human intestine. Science 307, 1915–1920. https://doi.org/10.1126/science.1104816.

Berry, M.D., 2004. Mammalian central nervous system trace amines. Pharmacologic amphetamines, physiologic neuromodulators. J. Neurochem. 90, 257–271. https://doi.org/10.1111/j.1471-4159.2004.02501.x.

Bhagwat, P.K., Dandge, P.B., 2018. Collagen and collagenolytic proteases: a review. Biocatal. Agric. Biotechnol. 15, 43–55. https://doi.org/10.1016/j.bcab.2018.05.005.

Bhattarai, Y., Williams, B.B., Battaglioli, E.J., Whitaker, W.R., Till, L., Grover, M., Linden, D.R., Akiba, Y., Kandimalla, K.K., Zachos, N.C., Kaunitz, J.D., Sonnenburg, J. L., Fischbach, M.A., Farrugia, G., Kashyap, P.C., 2018. Gut microbiota-produced tryptamine activates an epithelial G-protein-coupled receptor to increase colonic secretion. Cell Host Microbe 23, 775–785.e5. https://doi.org/10.1016/j.chom.2018.05.004.

Chen, H., Nwe, P.-K., Yang, Y., Rosen, C.E., Bielecka, A.A., Kuchroo, M., Cline, G.W., Kruse, A.C., Ring, A.M., Crawford, J.M., Palm, N.W., 2019. A forward chemical genetic screen reveals gut microbiota metabolites that modulate host physiology. Cell 177, 1217–1231.e18. https://doi.org/10.1016/j.cell.2019.03.036.

Choi, Y., Han, S.-W., Kim, J.-S., Jang, Y., Shin, J.-S., 2021. Biochemical characterization and synthetic application of aromatic l-amino acid decarboxylase from Bacillus atrophaeus. Appl. Microbiol Biotechnol. 105, 2775–2785. https://doi.org/10.1007/s00253-021-11122-3.

Connil, N., Le Breton, Y., Dousset, X., Auffray, Y., Rincé, A., Prévost, H., 2002. Identification of the enterococcus faecalis tyrosine decarboxylase operon involved in tyramine production. Appl. Environ. Microbiol. 68, 3537–3544. https://doi.org/10.1128/AEM.68.7.3537-3544.2002.

Corr, S.C., Li, Y., Riedel, C.U., O'Toole, P.W., Hill, C., Gahan, C.G.M., 2007. Bacteriocin production as a mechanism for the antiinfective activity of Lactobacillus salivarius UCC118. Proc. Natl. Acad. Sci. 104, 7617–7621. https://doi.org/10.1073/pnas.0700440104.

Cryan, J.F., O'Riordan, K.J., Cowan, C.S.M., Sandhu, K.V., Bastiaanssen, T.F.S., Boehme, M., Codagnone, M.G., Cussotto, S., Fulling, C., Golubeva, A.V., Guzzetta, K. E., Jaggar, M., Long-Smith, C.M., Lyte, J.M., Martin, J.A., Molinero-Perez, A., Moloney, G., Morelli, E., Morillas, E., O'Connor, R., Cruz-Pereira, J.S., Peterson, V.L., Rea, K., Ritz, N.L., Sherwin, E., Spichak, S., Teichman, E.M., van de Wouw, M., Ventura-Silva, A.P., Wallace-Fitzsimons, S.E., Hyland, N., Clarke, G., Dinan, T.G., 2019. The microbiota-gut-brain axis. Physiol. Rev. 99, 1877–2013. https://doi.org/10.1152/physrev.00018.2018.

Donia, M.S., Fischbach, M.A., 2015. Small molecules from the human microbiota. Science 349, 1254766. https://doi.org/10.1126/science.1254766.

Faith, J.J., Guruge, J.L., Charbonneau, M., Subramanian, S., Seedorf, H., Goodman, A.L., Clemente, J.C., Knight, R., Heath, A.C., Leibel, R.L., Rosenbaum, M., Gordon, J.I., 2013. The Long-Term Stability of the Human Gut Microbiota. Science 341, 1237439. https://doi.org/10.1126/science.1237439.

Fernandez, I.M., Silva, M., Schuch, R., Walker, W.A., Siber, A.M., Maurelli, A.T., McCormick, B.A., 2001. Cadaverine prevents the escape of shigella flexneri from the phagolysosome: a connection between bacterial dissemination and neutrophil transepithelial signaling. J. Infect. Dis. 184, 743–753. https://doi.org/10.1086/323035.

Fernandez-Cantos, M.V., Garcia-Morena, D., Iannone, V., El-Nezami, H., Kolehmainen, M., Kuipers, O.P., 2021. Role of microbiota and related metabolites in gastrointestinal tract barrier function in NAFLD. Tissue Barriers 0, 1879719. https://doi.org/10.1080/21688370.2021.1879719.

Fiorani, M., Del Vecchio, L.E., Dargenio, P., Kaitsas, F., Rozera, T., Porcari, S., Gasbarrini, A., Cammarota, G., Ianiro, G., 2023. Histamine-producing bacteria and their role in gastrointestinal disorders. Expert Rev. Gastroenterol. Hepatol. 17, 709–718. https://doi.org/10.1080/17474124.2023.2230865.

Gaines, S., van Praagh, J.B., Williamson, A.J., Jacobson, R.A., Hyoju, S., Zaborin, A., Mao, J., Koo, H.Y., Alpert, L., Bissonnette, M., Weichselbaum, R., Gilbert, J., Chang, E., Hyman, N., Zaborina, O., Shogan, B.D., Alverdy, J.C., 2020. Western diet promotes intestinal colonization by collagenolytic microbes and promotes tumor formation after colorectal surgery. Gastroenterology 158, 958–970.e2. https://doi.org/10.1053/j.gastro.2019.10.020.

Garcia-Morena, D., Fernandez-Cantos, M.V., Escalera, S.L., Lok, J., Iannone, V., Cancellieri, P., Maathuis, W., Panagiotou, G., Aranzamendi, C., Aidy, S.E., Kolehmainen, M., El-Nezami, H., Wellejus, A., Kuipers, O.P., 2024. In vitro influence of specific bacteroidales strains on gut and liver health related to metabolic dysfunction-associated fatty liver disease. Probiotics Antimicro. Prot. https://doi.org/10.1007/s12602-024-10219-1.

Gika, H., Virgiliou, C., Theodoridis, G., Plumb, R.S., Wilson, I.D., 2019. Untargeted LC/MS-based metabolic phenotyping (metabonomics/metabolomics): the state of the art. J. Chromatogr. B 1117, 136–147. https://doi.org/10.1016/j.jchromb.2019.04.009.

Gotoh, A., Nara, M., Sugiyama, Y., Sakanaka, M., Yachi, H., Kitakata, A., Nakagawa, A., Minami, H., Okuda, S., Katoh, T., Katayama, T., Kurihara, S., 2017. Use of Gifu Anaerobic Medium for culturing 32 dominant species of human gut microbes and its evaluation based on short-chain fatty acids fermentation profiles. Biosci., Biotechnol., Biochem. 81, 2009–2017. https://doi.org/10.1080/09168451.2017.1359486.

Guijas, C., Montenegro-Burke, J.R., Domingo-Almenara, X., Palermo, A., Warth, B., Hermann, G., Koellensperger, G., Huan, T., Uritboonthai, W., Aisporna, A.E., Wolan, D.W., Spilker, M.E., Benton, H.P., Siuzdak, G., 2018. METLIN: A Technology Platform for Identifying Knowns and Unknowns. Anal. Chem. 90, 3156–3164. https://doi.org/10.1021/acs.analchem.7b04424.

Haenisch, B., von Kügelgen, I., Bönisch, H., Göthert, M., Sauerbruch, T., Schepke, M., Marklein, G., Höfling, K., Schröder, D., Molderings, G.J., 2008. Regulatory mechanisms underlying agmatine homeostasis in humans. Am. J. Physiol. -Gastrointest. Liver Physiol. 295, G1104–G1110. https://doi.org/10.1152/ajpgi.90374.2008.

Han, S.-W., Shin, J.-S., 2022. Aromatic L-amino acid decarboxylases: mechanistic features and microbial applications. Appl. Microbiol Biotechnol. 106, 4445–4458. https://doi.org/10.1007/s00253-022-12028-4.

Hersh, B.M., Farooq, F.T., Barstad, D.N., Blankenhorn, D.L., Slonczewski, J.L., 1996. A glutamate-dependent acid resistance gene in Escherichia coli. J. Bacteriol. 178, 3978–3981. https://doi.org/10.1128/jb.178.13.3978-3981.1996.

Horvath, T.D., Ihekweazu, F.D., Haidacher, S.J., Ruan, W., Engevik, K.A., Fultz, R., Hoch, K.M., Luna, R.A., Oezguen, N., Spinler, J.K., Haag, A.M., Versalovic, J., Engevik, M.A., 2022. Bacteroides ovatus colonization influences the abundance of intestinal short chain fatty acids and neurotransmitters. iScience 25, 104158. https://doi.org/10.1016/j.isci.2022.104158.

Iyer, R., Williams, C., Miller, C., 2003. Arginine-Agmatine Antiporter in Extreme Acid Resistance in Escherichia coli. J. Bacteriol. 185, 6556–6561. https://doi.org/10.1128/jb.185.22.6556-6561.2003.

Johnson, C.H., Ivanisevic, J., Siuzdak, G., 2016. Metabolomics: beyond biomarkers and towards mechanisms. Nat. Rev. Mol. Cell Biol. 17, 451–459. https://doi.org/10.1038/nrm.2016.25.

Kanehisa, M., Goto, S., 2000. KEGG: Kyoto Encyclopedia of Genes and Genomes. Nucleic Acids Res. 28, 27–30. https://doi.org/10.1093/nar/28.1.27.
van Kessel, S.P., Frye, A.K., El-Gendy, A.O., Castejon, M., Keshavarzian, A., van Dijk, G., El Aidy, S., 2019. Gut bacterial tyrosine decarboxylases restrict levels of levodopa in the treatment of Parkinson's disease. Nat. Commun. 10, 310. https://doi.org/10.1038/s41467-019-08294-y.
Kezmarsky, N.D., Xu, H., Graham, D.E., White, R.H., 2005. Identification and characterization of a l-tyrosine decarboxylase in Methanocaldococcus jannaschii. Biochim. Et. Biophys. Acta (BBA) - Gen. Subj. 1722, 175–182. https://doi.org/10.1016/j.bbagen.2004.12.003.
Khan, M. zahid, Nawaz, W., 2016. The emerging roles of human trace amines and human trace amine-associated receptors (hTAARs) in central nervous system. Biomed. Pharmacother. 83, 439–449. https://doi.org/10.1016/j.biopha.2016.07.002.
Kim, S., Thiessen, P.A., Bolton, E.E., Chen, J., Fu, G., Gindulyte, A., Han, L., He, J., He, S., Shoemaker, B.A., Wang, J., Yu, B., Zhang, J., Bryant, S.H., 2016. PubChem Substance and Compound databases. Nucleic Acids Res. 44, D1202–D1213. https://doi.org/10.1093/nar/gkv951.
Klåvus, A., Kokla, M., Noerman, S., Koistinen, V.M., Tuomainen, M., Zarei, I., Meuronen, T., Häkkinen, M.R., Rummukainen, S., Farizah Babu, A., Sallinen, T., Kärkkäinen, O., Paananen, J., Broadhurst, D., Brunius, C., Hanhineva, K., 2020. Notame": Workflow for Non-Targeted LC–MS Metabolic Profiling. Metabolites 10, 135. https://doi.org/10.3390/metabo10040135.
Koistinen, V.M., Kärkkäinen, O., Borewicz, K., Zarei, I., Jokkala, J., Micard, V., Rosa-Sibakov, N., Auriola, S., Aura, A.-M., Smidt, H., Hanhineva, K., 2019. Contribution of gut microbiota to metabolism of dietary glycine betaine in mice and in vitro colonic fermentation. Microbiome 7, 103. https://doi.org/10.1186/s40168-019-0718-2.
Korem, T., Zeevi, D., Suez, J., Weinberger, A., Avnit-Sagi, T., Pompan-Lotan, M., Matot, E., Jona, G., Harmelin, A., Cohen, N., Sirota-Madi, A., Thaiss, C.A., Pevsner-Fischer, M., Sorek, R., Xavier, R.J., Elinav, E., Segal, E., 2015. Growth dynamics of gut microbiota in health and disease inferred from single metagenomic samples. Science 349, 1101–1106. https://doi.org/10.1126/science.aac4812.
Kovács, T., Mikó, E., Vida, A., Sebő, É., Toth, J., Csonka, T., Boratkó, A., Ujlaki, G., Lente, G., Kovács, P., Tóth, D., Árkosy, P., Kiss, B., Méhes, G., Goedert, J.J., Bai, P., 2019. Cadaverine, a metabolite of the microbiome, reduces breast cancer aggressiveness through trace amino acid receptors. Sci. Rep. 9, 1300. https://doi.org/10.1038/s41598-018-37664-7.
Levine, M., Lohinai, Z.M., 2021. Resolving the contradictory functions of lysine decarboxylase and butyrate in periodontal and intestinal diseases. J. Clin. Med 10, 2360. https://doi.org/10.3390/jcm10112360.
Lim, J.J., Diener, C., Wilson, J., Valenzuela, J.J., Baliga, N.S., Gibbons, S.M., 2023. Growth phase estimation for abundant bacterial populations sampled longitudinally from human stool metagenomes. Nat. Commun. 14, 5682. https://doi.org/10.1038/s41467-023-41424-1.
Liu, J., Tan, Y., Cheng, H., Zhang, D., Feng, W., Peng, C., 2022. Functions of gut microbiota metabolites, current status and future perspectives. Aging Dis. 13, 1106–1126. https://doi.org/10.14336/AD.2022.0104.
Mazmanian, S.K., Round, J.L., Kasper, D.L., 2008. A microbial symbiosis factor prevents intestinal inflammatory disease. Nature 453, 620–625. https://doi.org/10.1038/nature07008.
McCormick, B.A., Fernandez, M.I., Siber, A.M., Maurelli, A.T., 1999. Inhibition of Shigella flexneri-induced transepithelial migration of polymorphonuclear leucocytes by cadaverine. Cell. Microbiol. 1, 143–155. https://doi.org/10.1046/j.1462-5822.1999.00014.x.
Meadows, J.A., Wargo, M.J., 2015. Carnitine in bacterial physiology and metabolism. Microbiology 161, 1161. https://doi.org/10.1099/mic.0.000080.
Metsalu, T., Vilo, J., 2015. ClustVis: a web tool for visualizing clustering of multivariate data using Principal Component Analysis and heatmap. W566–W570 Nucleic Acids Res. 43. https://doi.org/10.1093/nar/gkv468.
Miller, G.M., 2011. The emerging role of trace amine-associated receptor 1 in the functional regulation of monoamine transporters and dopaminergic activity. J. Neurochem. 116, 164–176. https://doi.org/10.1111/j.1471-4159.2010.07109.x.
Moreno-Arribas, V., Lonvaud-Funel, A., 2001. Purification and characterization of tyrosine decarboxylase of Lactobacillus brevis IOEB 9809 isolated from wine. FEMS Microbiol Lett. 195, 103–107. https://doi.org/10.1111/j.1574-6968.2001.tb10505.x.
Ni, Y., Qian, L., Siliceo, S.L., Long, X., Nychas, E., Liu, Y., Ismaiah, M.J., Leung, H., Zhang, L., Gao, Q., Wu, Q., Zhang, Y., Jia, X., Liu, S., Yuan, R., Zhou, L., Wang, X., Li, Q., Zhao, Y., El-Nezami, H., Xu, A., Xu, G., Li, H., Panagiotou, G., Jia, W., 2023. Resistant starch decreases intrahepatic triglycerides in patients with NAFLD via gut microbiome alterations. e8 Cell Metab. 35, 1530–1547. https://doi.org/10.1016/j.cmet.2023.08.002.
Nissim, Itzhak, Horyn, O., Daikhin, Y., Chen, P., Li, C., Wehrli, S.L., Nissim, Ilana, Yudkoff, M., 2014. The Molecular and Metabolic Influence of Long Term Agmatine Consumption *. J. Biol. Chem. 289, 9710–9729. https://doi.org/10.1074/jbc.M113.544726.
Pang, Z., Zhou, G., Ewald, J., Chang, L., Hacariz, O., Basu, N., Xia, J., 2022. Using MetaboAnalyst 5.0 for LC–HRMS spectra processing, multi-omics integration and covariate adjustment of global metabolomics data. Nat. Protoc. 17, 1735–1761. https://doi.org/10.1038/s41596-022-00710-w.
Parsons, M.E., Ganellin, C.R., 2006. Histamine and its receptors. Br. J. Pharmacol. 147, S127–S135. https://doi.org/10.1038/sj.bjp.0706440.
Pedersen, H.K., Gudmundsdottir, V., Nielsen, H.B., Hyotylainen, T., Nielsen, T., Jensen, B.A.H., Forslund, K., Hildebrand, F., Prifti, E., Falony, G., Le Chatelier, E., Levenez, F., Doré, J., Mattila, I., Plichta, D.R., Pöhö, P., Hellgren, L.I., Arumugam, M., Sunagawa, S., Vieira-Silva, S., Jørgensen, T., Holm, J.B., Trošt, K., Consortium, M., Kristiansen, K., Brix, S., Raes, J., Wang, J., Hansen, T., Bork, P., Brunak, S., Oresic, M., Ehrlich, S.D., Pedersen, O., 2016. Human gut microbes impact host serum metabolome and insulin sensitivity. Nature 535, 376–381. https://doi.org/10.1038/nature18646.
Pedley, A.M., Benkovic, S.J., 2017. A New View into the Regulation of Purine Metabolism – The Purinosome. Trends Biochem Sci. 42, 141–154. https://doi.org/10.1016/j.tibs.2016.09.009.
Pereira, C.I., Matos, D., San Romão, M.V., Crespo, M.T.B., 2009. Dual role for the tyrosine decarboxylation pathway in Enterococcus faecium E17: response to an acid challenge and generation of a proton motive force. Appl. Environ. Microbiol 75, 345–352. https://doi.org/10.1128/AEM.01958-08.
Perez, M., Calles-Enríquez, M., Nes, I., Martin, M.C., Fernandez, M., Ladero, V., Alvarez, M.A., 2015. Tyramine biosynthesis is transcriptionally induced at low pH and improves the fitness of Enterococcus faecalis in acidic environments. Appl. Microbiol Biotechnol. 99, 3547–3558. https://doi.org/10.1007/s00253-014-6301-7.
Qi, H., Li, Y., Yun, H., Zhang, T., Huang, Y., Zhou, J., Yan, H., Wei, J., Liu, Y., Zhang, Z., Gao, Y., Che, Y., Su, X., Zhu, D., Zhang, Y., Zhong, J., Yang, R., 2019. Lactobacillus maintains healthy gut mucosa by producing L-Ornithine. Commun. Biol. 2, 1–14. https://doi.org/10.1038/s42003-019-0424-4.
Qin, J., Li, R., Raes, J., Arumugam, M., Burgdorf, K.S., Manichanh, C., Nielsen, T., Pons, N., Levenez, F., Yamada, T., Mende, D.R., Li, J., Xu, J., Li, Shaochuan, Li, D., Cao, J., Wang, B., Liang, H., Zheng, H., Xie, Y., Tap, J., Lepage, P., Bertalan, M., Batto, J.-M., Hansen, T., Le Paslier, D., Linneberg, A., Nielsen, H.B., Pelletier, E., Renault, P., Sicheritz-Ponten, T., Turner, K., Zhu, H., Yu, C., Li, Shengting, Jian, M., Zhou, Y., Li, Y., Zhang, X., Li, Songgang, Qin, N., Yang, H., Wang, Jian, Brunak, S., Doré, J., Guarner, F., Kristiansen, K., Pedersen, O., Parkhill, J., Weissenbach, J., Bork, P., Ehrlich, S.D., Wang, 2010. A human gut microbial gene catalogue established by metagenomic sequencing (Jun,). Nature 464, 59–65. https://doi.org/10.1038/nature08821.
Ramakrishna, C., Kujawski, M., Chu, H., Li, L., Mazmanian, S.K., Cantin, E.M., 2019. Bacteroides fragilis polysaccharide A induces IL-10 secreting B and T cells that prevent viral encephalitis. Nat. Commun. 10, 2153. https://doi.org/10.1038/s41467-019-09884-6.
Ramos-Molina, B., Queipo-Ortuño, M.I., Lambertos, A., Tinahones, F.J., Peñafiel, R., 2019. Dietary and Gut Microbiota Polyamines in Obesity- and Age-Related Diseases. Front. Nutr. 6.
Ramshaw, J.A.M., Shah, N.K., Brodsky, B., 1998. Gly-X-Y Tripeptide Frequencies in Collagen: A Context for Host–Guest Triple-Helical Peptides. J. Struct. Biol. 122, 86–91. https://doi.org/10.1006/jsbi.1998.3977.
Rettedal, E.A., Gumpert, H., Sommer, M.O.A., 2014. Cultivation-based multiplex phenotyping of human gut microbiota allows targeted recovery of previously uncultured bacteria. Nat. Commun. 5, 4714. https://doi.org/10.1038/ncomms5714.
Reyes, A., Haynes, M., Hanson, N., Angly, F.E., Heath, A.C., Rohwer, F., Gordon, J.I., 2010. Viruses in the faecal microbiota of monozygotic twins and their mothers. Nature 466, 334–338. https://doi.org/10.1038/nature09199.
Roelofs, K.G., Coyne, M.J., Gentyala, R.R., Chatzidaki-Livanis, M., Comstock, L.E., 2016. Bacteroidales secreted antimicrobial proteins target surface molecules necessary for gut colonization and mediate competition in vivo. mBio 7. https://doi.org/10.1128/mBio.01055-16.
Round, J.L., Mazmanian, S.K., 2010. Inducible Foxp3+ regulatory T-cell development by a commensal bacterium of the intestinal microbiota. Proc. Natl. Acad. Sci. 107, 12204–12209. https://doi.org/10.1073/pnas.0909122107.
Saha, P., Panda, S., Holkar, A., Vashishth, R., Rana, S.S., Arumugam, M., Ashraf, G.M., Haque, S., Ahmad, F., 2023. Neuroprotection by agmatine: Possible involvement of the gut microbiome? Ageing Res. Rev. 91, 102056 https://doi.org/10.1016/j.arr.2023.102056.
Schwarz, J., Schumacher, K., Brameyer, S., Jung, K., 2022. Bacterial battle against acidity. FEMS Microbiol. Rev. 46, fuac037 https://doi.org/10.1093/femsre/fuac037.
Seim, H., Löster, H., Claus, R., Kleber, H.-P., Strack, E., 1982. Stimulation of the anaerobic growth ofSalmonella typhimurium by reduction ofl-carnitine, carnitine derivatives and structure-related trimethylammonium compounds. Arch. Microbiol. 132, 91–95. https://doi.org/10.1007/BF00690825.
Semba, R.D., Trehan, I., Li, X., Moaddel, R., Ordiz, M.I., Maleta, K.M., Kraemer, K., Shardell, M., Ferrucci, L., Manary, M., 2017. Environmental Enteric Dysfunction is Associated with Carnitine Deficiency and Altered Fatty Acid Oxidation. eBioMedicine 17, 57–66. https://doi.org/10.1016/j.ebiom.2017.01.026.
Shibasaki, T., Mori, H., Chiba, S., Ozaki, A., 1999. Microbial proline 4-hydroxylase screening and gene cloning. Appl. Environ. Microbiol. 65, 4028–4031. https://doi.org/10.1128/AEM.65.9.4028-4031.1999.
Shoulders, M.D., Raines, R.T., 2009. Collagen Structure and Stability. Annu. Rev. Biochem. 78, 929–958. https://doi.org/10.1146/annurev.biochem.77.032207.120833.
Shrode, R.L., Knobbe, J.E., Cady, N., Yadav, M., Hoang, J., Cherwin, C., Curry, M., Garje, R., Vikas, P., Sugg, S., Phadke, S., Filardo, E., Mangalam, A.K., 2023. Breast cancer patients from the Midwest region of the United States have reduced levels of short-chain fatty acid-producing gut bacteria. Sci. Rep. 13, 526. https://doi.org/10.1038/s41598-023-27436-3.
Smith, C.A., Maille, G.O., Want, E.J., Qin, C., Trauger, S.A., Brandon, T.R., Custodio, D. E., Abagyan, R., Siuzdak, G., 2005. METLIN: A Metabolite Mass Spectral Database. Ther. Drug Monit. 27, 747. https://doi.org/10.1097/01.ftd.0000179845.53213.39.
Strandwitz, P., Kim, K.H., Terekhova, D., Liu, J.K., Sharma, A., Levering, J., McDonald, D., Dietrich, D., Ramadhar, T.R., Lekbua, A., Mroue, N., Liston, C., Stewart, E.J., Dubin, M.J., Zengler, K., Knight, R., Gilbert, J.A., Clardy, J., Lewis, K., 2019. GABA-modulating bacteria of the human gut microbiota. Nat. Microbiol 4, 396–403. https://doi.org/10.1038/s41564-018-0307-3.

Sumner, L.W., Amberg, A., Barrett, D., Beale, M.H., Beger, R., Daykin, C.A., Fan, T.W.-M., Fiehn, O., Goodacre, R., Griffin, J.L., Hankemeier, T., Hardy, N., Harnly, J., Higashi, R., Kopka, J., Lane, A.N., Lindon, J.C., Marriott, P., Nicholls, A.W., Reily, M. D., Thaden, J.J., Viant, M.R., 2007. Proposed minimum reporting standards for chemical analysis. Metabolomics 3, 211–221. https://doi.org/10.1007/s11306-007-0082-2.

Takahashi, N., Kato, T., Kuramitsu, H.K., 1991. Isolation and preliminary characterization of the Porphyromonas gingivalis prtC gene expressing collagenase activity. FEMS Microbiol. Lett. 84, 135–138. https://doi.org/10.1111/j.1574-6968.1991.tb04585.x.

Tramontano, M., Andrejev, S., Pruteanu, M., Klünemann, M., Kuhn, M., Galardini, M., Jouhten, P., Zelezniak, A., Zeller, G., Bork, P., Typas, A., Patil, K.R., 2018. Nutritional preferences of human gut bacteria reveal their metabolic idiosyncrasies. Nat. Microbiol 3, 514–522. https://doi.org/10.1038/s41564-018-0123-9.

Tripathi, A., Debelius, J., Brenner, D.A., Karin, M., Loomba, R., Schnabl, B., Knight, R., 2018. The gut-liver axis and the intersection with the microbiome. Nat. Rev. Gastroenterol. Hepatol. 15, 397–411. https://doi.org/10.1038/s41575-018-0011-z.

Tsugawa, H., Cajka, T., Kind, T., Ma, Y., Higgins, B., Ikeda, K., Kanazawa, M., VanderGheynst, J., Fiehn, O., Arita, M., 2015. MS-DIAL: data-independent MS/MS deconvolution for comprehensive metabolome analysis. Nat. Methods 12, 523–526. https://doi.org/10.1038/nmeth.3393.

Tsugawa, H., Kind, T., Nakabayashi, R., Yukihira, D., Tanaka, W., Cajka, T., Saito, K., Fiehn, O., Arita, M., 2016. Hydrogen Rearrangement Rules: Computational MS/MS Fragmentation and Structure Elucidation Using MS-FINDER Software. Anal. Chem. 88, 7946–7958. https://doi.org/10.1021/acs.analchem.6b00770.

Waclawiková, B., Bullock, A., Schwalbe, M., Aranzamendi, C., Nelemans, S.A., Dijk, G., van, Aidy, S.E., 2021. Gut bacteria-derived 5-hydroxyindole is a potent stimulant of intestinal motility via its action on L-type calcium channels. PLoS Biol. 19, e3001070 https://doi.org/10.1371/journal.pbio.3001070.

Wexler, H.M., 2007. Bacteroides: the good, the bad, and the nitty-gritty. Clin. Microbiol. Rev. 20, 593–621. https://doi.org/10.1128/cmr.00008-07.

Williams, B.B., Van Benschoten, A.H., Cimermancic, P., Donia, M.S., Zimmermann, M., Taketani, M., Ishihara, A., Kashyap, P.C., Fraser, J.S., Fischbach, M.A., 2014. Discovery and characterization of gut microbiota decarboxylases that can produce the neurotransmitter tryptamine. Cell Host Microbe 16, 495–503. https://doi.org/10.1016/j.chom.2014.09.001.

Williamson, A.J., Jacobson, R., van Praagh, J.B., Gaines, S., Koo, H.Y., Lee, B., Chan, W.-C., Weichselbaum, R., Alverdy, J.C., Zaborina, O., Shogan, B.D., 2022. Enterococcus faecalis promotes a migratory and invasive phenotype in colon cancer cells. Neoplasia 27, 100787. https://doi.org/10.1016/j.neo.2022.100787.

Wishart, D.S., Tzur, D., Knox, C., Eisner, R., Guo, A.C., Young, N., Cheng, D., Jewell, K., Arndt, D., Sawhney, S., Fung, C., Nikolai, L., Lewis, M., Coutouly, M.-A., Forsythe, I., Tang, P., Shrivastava, S., Jeroncic, K., Stothard, P., Amegbey, G., Block, D., Hau, DavidD., Wagner, J., Miniaci, J., Clements, M., Gebremedhin, M., Guo, N., Zhang, Y., Duggan, G.E., MacInnis, G.D., Weljie, A.M., Dowlatabadi, R., Bamforth, F., Clive, D., Greiner, R., Li, L., Marrie, T., Sykes, B.D., Vogel, H.J., Querengesser, L., 2007. HMDB: the human metabolome database. Nucleic Acids Res. 35, D521–D526. https://doi.org/10.1093/nar/gkl923.

Wolken, W.A.M., Lucas, P.M., Lonvaud-Funel, A., Lolkema, J.S., 2006. The mechanism of the tyrosine transporter TyrP supports a proton motive tyrosine decarboxylation pathway in lactobacillus brevis. J. Bacteriol. 188, 2198–2206. https://doi.org/10.1128/jb.188.6.2198-2206.2006.

Yamauchi, M., Shiiba, M., 2008. Lysine Hydroxylation and Cross-linking of Collagen. In: Kannicht, C. (Ed.), Post-Translational Modifications of Proteins: Tools for Functional Proteomics, Methods in Molecular Biology™. Humana Press, Totowa, NJ, pp. 95–108. https://doi.org/10.1007/978-1-60327-084-7_7.

Yano, J.M., Yu, K., Donaldson, G.P., Shastri, G.G., Ann, P., Ma, L., Nagler, C.R., Ismagilov, R.F., Mazmanian, S.K., Hsiao, E.Y., 2015. Indigenous bacteria from the gut microbiota regulate host serotonin biosynthesis. Cell 161, 264–276. https://doi.org/10.1016/j.cell.2015.02.047.

Yoshimoto, S., Loo, T.M., Atarashi, K., Kanda, H., Sato, S., Oyadomari, S., Iwakura, Y., Oshima, K., Morita, H., Hattori, M., Honda, K., Ishikawa, Y., Hara, E., Ohtani, N., 2013. Obesity-induced gut microbial metabolite promotes liver cancer through senescence secretome. Nature 499, 97–101. https://doi.org/10.1038/nature12347.

Yuan, M., Breitkopf, S.B., Yang, X., Asara, J.M., 2012. A positive/negative ion–switching, targeted mass spectrometry–based metabolomics platform for bodily fluids, cells, and fresh and fixed tissue. Nat. Protoc. 7, 872–881. https://doi.org/10.1038/nprot.2012.024.

Zafar, H., Saier, M.H., 2021. Gut Bacteroides species in health and disease. Gut Microbes 13, 1848158. https://doi.org/10.1080/19490976.2020.1848158.

Zarei, I., Koistinen, V.M., Kokla, M., Klåvus, A., Babu, A.F., Lehtonen, M., Auriola, S., Hanhineva, K., 2022. Tissue-wide metabolomics reveals wide impact of gut microbiota on mice metabolite composition. Sci. Rep. 12, 15018 https://doi.org/10.1038/s41598-022-19327-w.

Zhai, L., Xiao, H., Lin, C., Wong, H.L.X., Lam, Y.Y., Gong, M., Wu, G., Ning, Z., Huang, C., Zhang, Y., Yang, C., Luo, J., Zhang, L., Zhao, Ling, Zhang, C., Lau, J.Y.-N., Lu, A., Lau, L.-T., Jia, W., Zhao, Liping, Bian, Z.-X., 2023. Gut microbiota-derived tryptamine and phenethylamine impair insulin sensitivity in metabolic syndrome and irritable bowel syndrome. Nat. Commun. 14, 4986. https://doi.org/10.1038/s41467-023-40552-y.

Zhang, Z., Liu, P., Su, W., Zhang, H., Xu, W., Chu, X., 2021. Metabolic engineering strategy for synthetizing trans-4-hydroxy-l-proline in microorganisms. Micro Cell Fact. 20 (1), 15. https://doi.org/10.1186/s12934-021-01579-2.